Article:

Current Saturation Behavior in GaN Polarization Superjunction Hybrid Diode

Yangming Du, Ekkanath Madathil Sankara Narayanan,* Hiroji Kawai, Shuichi Yagi, and Hironobu Narui

This is the first report on the current saturation behavior observed in the forward characteristics of polarization superjunction (PSJ)-based hybrid PiN-Schottky GaN power diodes fabricated on Sapphire. In the current saturation region, most of the applied anode voltage is dropped across the regions immediately adjacent to the edge of the doped P-GaN region closest to the cathode. This significant potential drop occurs within a short distance, resulting in a high electric field and depletion of electrons, causing the current saturation behavior via velocity saturation in these PSJ hybrid diodes.

1. Introduction

Gallium nitride (GaN) has become an essential candidate as the next-generation semiconductor material for power devices because of its higher bandgap energy than silicon or silicon carbide. The high density of 2D electron gas (2DEG) formed at the aluminum gallium nitride (AlGaN)/GaN heterostructures interface[1] has high mobility (around $1500 \, \mathrm{cm^2 \, Vs^{-1}}$)[2] and high saturation velocity. Due to these features, GaN power devices can achieve lower specific on-state resistance than Si and SiC devices[3] for a given breakdown voltage.

Polarization superjunction (PSJ) is a concept utilizing the formation of high-density 2D hole gas (2DHG)[4–6] coexisting with high-density 2DEG in a double heterostructure of GaN/AlGaN/GaN, which can achieve charge balance condition and flat electric field distribution, thus significantly improving the breakdown voltage for a given drift region length.[7–13] Analysis of the PSJ concept is also independently reported by others.[14,15] A 2.4 kV lateral PSJ hybrid diode on 6 H-SiC substrate was first reported in ref. [10]. It is a merged Schottky and PiN diode. Due to the advantages of PSJ technologies, the diodes can achieve a low on-set voltage (0.4 V), high reverse blocking voltage (around 2.4 kV), and specific on-state resistance of $R_{on} \cdot A = 14 \, \mathrm{m\Omega \, cm^2}$ at room temperature. This work also showed the capacitance performances of PSJ hybrid diodes, indicating that the Schottky junction was depleted first followed by the depletion of the PiN junction (2DEG/2DHG) under high reverse bias conditions. Furthermore, the surge current capability of the PSJ hybrid diode on insulating Sapphire substrate has also been reported in ref. [16]. The measured surge current was around around 8 times its rated current (8A). When the high surge current flows through Schottky Anode, the high potential drop will cause the turn-on of the PiN junction in PSJ hybrid diode. Therefore, the highly energetic minority carriers (holes) are injected through the PiN junction under very high forward bias at high temperatures, inducing lattice damage and device burnout.[16] As for the switching performances of PSJ devices, the electrons and holes can be depleted/supplemented through the drain and gate in PSJ heterostructure field-effect transistors (HFETs) (cathode and p-type anode in PSJ diode) during the turn-off/turn-on process, respectively. This behavior has already been validated and reported in refs. [12,17,18].

The previous research work found a current saturation behavior that influenced the performances of these PSJ hybrid diodes, but the mechanisms were not discussed.[16] Therefore, the current saturation behavior observed and the mechanisms governing such behavior are discussed in this work.

Y. Du, E. M. Sankara Narayanan
Department of Electronic and Electrical Engineering
The University of Sheffield
Sir Frederick Mappin Building, Mappin Street, Sheffield S1 3JD, UK
E-mail: s.madathil@sheffield.ac.uk

H. Kawai, S. Yagi, H. Narui
Powdec K.K
1-23-15 Wakagi-cho, Oyama City, Tochigi 323-0028, Japan

2. Device Structure and Dimensions

The cross-section and dimensions of PSJ hybrid diodes are illustrated in **Figure 1**. PSJ double heterostructures (u-GaN/AlGaN/u-GaN) are capped with P++GaN layer to provide Ohmic contact to the anode (A), and the thicknesses are 30 nm, with Mg doping density of $\approx$1e20 and 1e19 $\mathrm{cm^{-3}}$, respectively. The thicknesses of the top and bottom u-GaN layers are 20 and 800 nm, respectively. AlGaN layer thickness is 25 nm, and the Al content is 0.3. Unlike the devices reported in ref. [10] or,[16] Schottky anode contacts are formed over the AlGaN layer, and PiN diodes are formed over GaN/AlGaN/GaN, with P-GaN/P + GaN forming the Ohmic anode to the 2DHG. The cathode is formed by contacting the 2DEG over the AlGaN layer, as shown in Figure 1. Therefore, high densities of 2DHG and 2DEG are formed at the top and
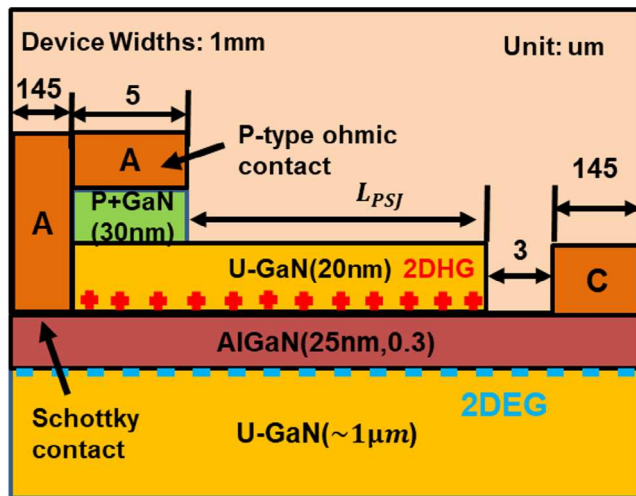
Figure 1. A simplified cross-section of PSJ hybrid diode. A and C represent the anode and cathode, respectively.

bottom interfaces of the double heterostructure of GaN/AlGaN/GaN, respectively. This device structure is same as that shown in the previous work.[10] Such a structure makes use of charge balance arising across the high-density 2DHG, AlGaN intrinsic layer, and high-density 2DEG in the drift region (Lpsj) to support (linearly varying) high voltages with drift regions for high-voltage applications. Other detailed dimensions of these diodes are presented in Figure 1. The widths of the devices under test are 1 mm.

3. Results and Discussions

3.1. Forward and Reverse Characteristics of GaN PSJ Hybrid Diodes

Measured forward I–V characteristics of PSJ hybrid diodes with different L_{PSJ} at room temperatures and in the dark are plotted in **Figure** 2a. The turn-on voltage is measured to be 1.6 V
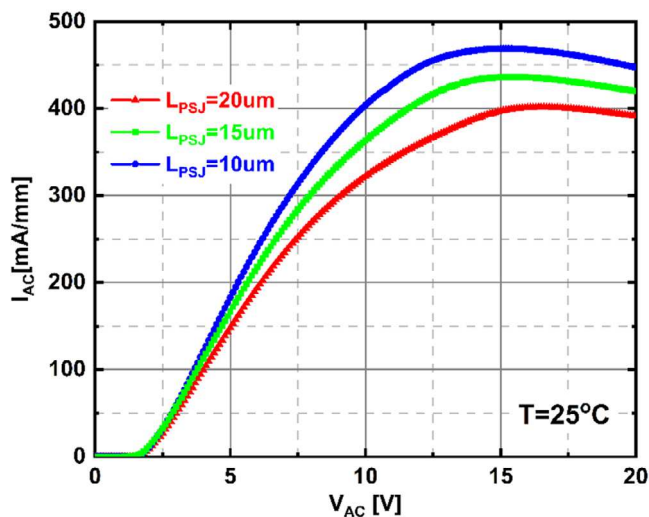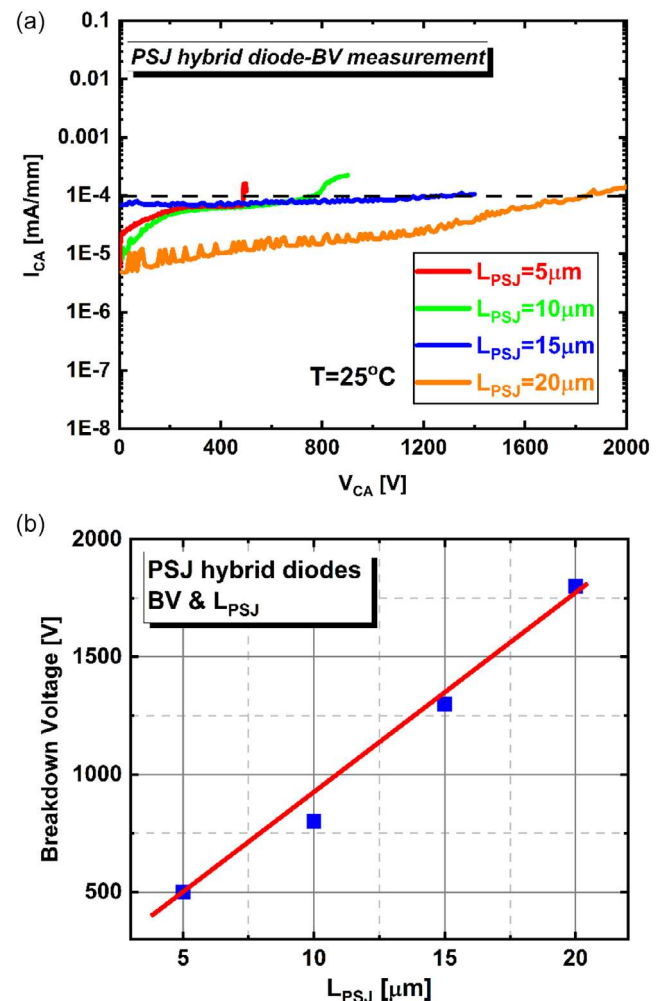

Figure 2. Measured forward characteristics of PSJ hybrid diodes with different diodes of $L_{PSJ} = 10$, 15, and 20 μm at room temperature.

(@1 mA mm^{-1}) at $T = 25$ °C in these devices. This is due to the fact that the Schottky contact is formed on the AlGaN layer. There are no limitations in electrons available to be injected across the Schottky barrier under the forward bias. However, the forward conductive characteristics have a current saturation behavior, and the saturation voltage is independent of the L_{PSJ}. This indicates that the saturation behavior does not depend on the length of the PSJ drift region.

Moreover, the current saturation behavior is widely observed from the conventional GaN high electron mobility transistors (HEMTs). This is due to the velocity saturation that occurred at the drain-side edge of the gate. When the device turns on, the electrons at this region are gradually accelerated when the drain bias increases, causing the velocity saturation at this region. However, the potential distribution of GaN HEMTs is different from that in PSJ hybrid diode under the same forward bias. Therefore, the actual mechanisms of this diode are discussed in further sections.

Measured breakdown voltages of these hybrid diodes with different L_{PSJ} (10, 15, and 20 μm) at room temperatures and in the dark are presented in **Figure 3**, which shows effective

Figure 3. a) Measured reverse characteristics of PSJ hybrid diode and b) the extracted breakdown voltage (@ 1e−4 mA mm^{-1}) with different $L_{PSJ} = 5$, 10, 15, and 20 μm.

polarized charge balance. Due to charge balance arising across the high-density 2DHG and high-density 2DEG, these devices exhibit high breakdown voltages, which vary linearly with drift lengths (L_{PSJ}), as shown in Figure 2b. These results were almost identical to that reported in ref. [10].

3.2. Simulation Analysis of Current Saturation Behavior in GaN PSJ Hybrid Diodes

To investigate the mechanisms governing current saturation in PSJ hybrid diode, device models are built in the SILVACO ATLAS based on the typical models in ref. [19]. The knee voltage, on-resistance, and saturation voltage of simulated results are well-fitted with the experimental results by modulating the density and mobility of 2DEG shown in **Figure 4**. The deviation at the saturation region between simulation and experimental results is due to self-heating effects not accounted for in the simulations. Moreover, the simulation results also indicate that the self-heating effects have negligible influences on this current saturation behavior.

3.2.1. Potential Distribution Along the 2DHG and 2DEG Channels

It is important to note that, although the PSJ hybrid diodes are merged with Schottky and PiN diodes, the PiN junctions do not turn on due to the low resistivity manner of 2DEG and relatively higher turn-on voltage of PiN junctions (3.4 V) when compared with the Schottky component of these diodes. The surge current measurement results of PSJ hybrid diodes also verified that the PiN junctions do not turn on when the anode bias is lower than 30 V at room temperature.[16] This indicates that this PSJ hybrid diode behaves as a unipolar power device and electrons are the main carriers at forward conducting mechanisms under normal operating conditions. In other words, the electrons flow through the Schottky anode and 2DEG channel into the cathode, which forms the major current flow in this diode.
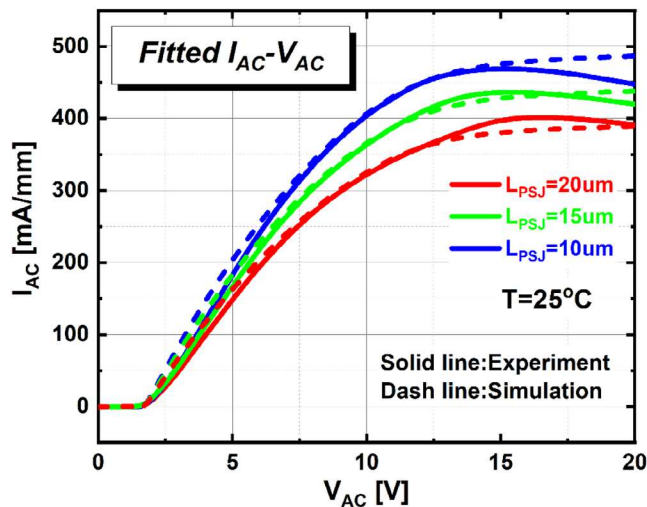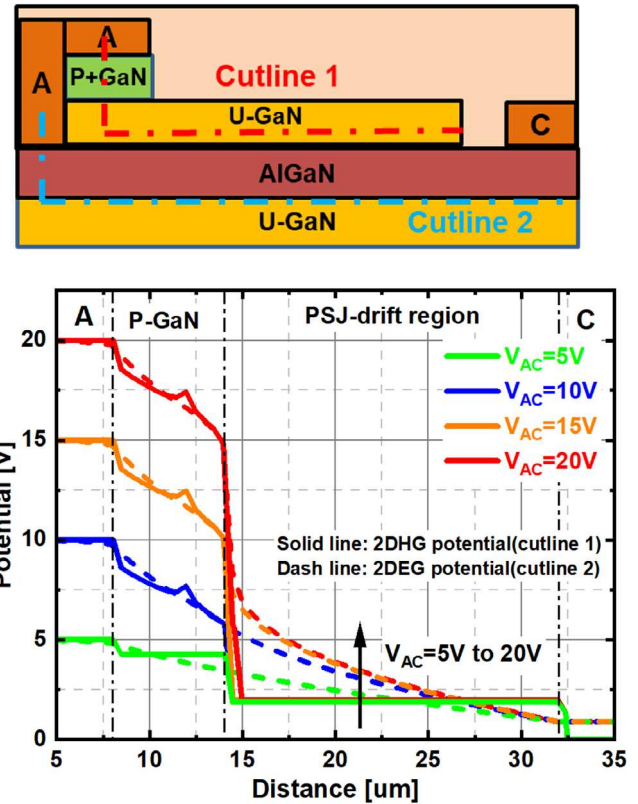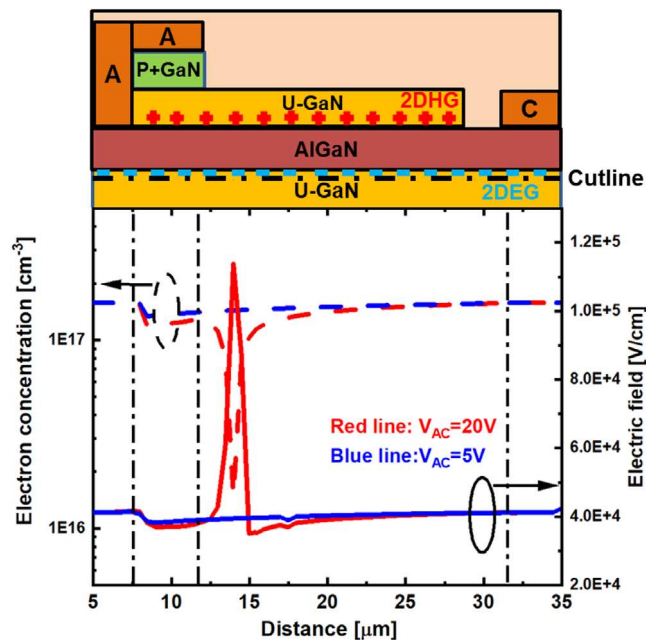

Figure 5. The cutline position (above) and the potential distribution along Cutline 1 and Cutline 2 range from $V_{AC} = 5$–20 V with the step of 5 V (below).

Figure 5 presents the potential distribution along 2DHG and 2DEG channels for both saturation and nonsaturation conditions along the Cutlines 1 and 2 at different anode biases with the $L_{PSJ} = 15\,\mu m$ and device lengths W = 1 mm. As is evident, the potential drops almost linearly in the P + GaN along the 2DHG channel. However, due to the high resistive of the top u-GaN layer (2DHG has a low velocity and is mainly confined at the heterointerface), the rest of the applied anode potential to be dropped across the regions immediately adjacent to the edge of the P + GaN region toward the cathode. This phenomenon is observed from both the nonsaturation and saturation situation but with the increasing voltage drop. This significant potential drop occurs within a short distance, resulting in the high electric field at the 2DEG channel close to the edge of the anode below the P + GaN region.

However, the potential distribution along the 2DEG channel is different. It can be found that the applied anode potential drop across the Schottky contact region is about 1.6 V in the saturation region along the 2DEG channel, which is consistent with the knee voltage presented in Figure 2. At the nonsaturation region ($V_{AC} = 5$ and 10 V), the potential drops almost linearly from the 2DEG channel below the P + GaN region, and the drift region (PSJ) has a very low potential drop due to the high density of 2DEG, which keeps the potential of the L_{PSJ} region as low as possible. At the nonsaturation region ($V_{AC} = 15$ and 20 V), although the potential drop rate at the 2DEG channel below the P + GaN region and the PSJ drift region is almost consistent, the potential drop at the edge of the anode becomes significant.

Figure 4. Fitted I_{AC}–V_{AC} characteristics of PSJ hybrid diodes with different L_{PSJ} (10, 15, and 20 μm).

Figure 6. Simulated total electric field and electron concentration distribution along the 2DEG channel at $V_{AC} = 5\,V$ (blue) and 20 V (red), respectively.

The top u-GaN layer behaves as a resistive layer, because the 2DHG has a low velocity and is mainly confined at the heterointerface. Therefore, the potential along Cutline 1 drops significantly horizontally. Moreover, the holes cannot be injected into the bottom u-GaN layer, which cannot increase the number of electrons in 2DEG channel.

Figure 6 presents the electric field and electron concentration along the 2DEG channel at anode biases of 5 V (not-saturation) and 20 V (saturation), respectively. Compared with the electric field distribution at 5 V, with an increase in bias to 20 V, the high electric field peak creates a pinch-off region, causing the depletion of 2DEG.

According to previous discussions on these mechanisms, the saturation behavior has almost no relationship with the PSJ region. This also explains why saturation voltage is independent of L_{PSJ} obtained from the measurement results shown in Figure 2. The detailed mechanisms of this saturation behavior in PSJ hybrid are illustrated in **Figure 7**. When the diode turns on, the current flows through the Schottky anode and 2DEG channel to the cathode. The potential along the 2DEG channel drops gradually. However, the potential at the edge of the p-Ohmic contact drops significantly. With the increase of the anode voltage, the potential differences and electric field peak are generated in that region. Therefore, the high electric field peak pinches off the 2DEG channel, which is close to the edge of the p-Ohmic anode shown in Figure 7.

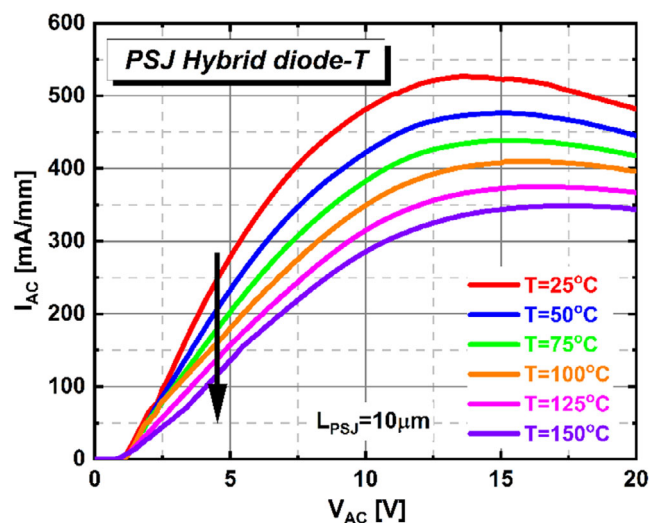### 3.3. Temperature-Dependent I–V Characteristics of GaN PSJ Hybrid Diodes

In this section, temperature-dependent I–V characteristics are presented and further explain the current saturation mechanisms obtained from the simulation analysis.
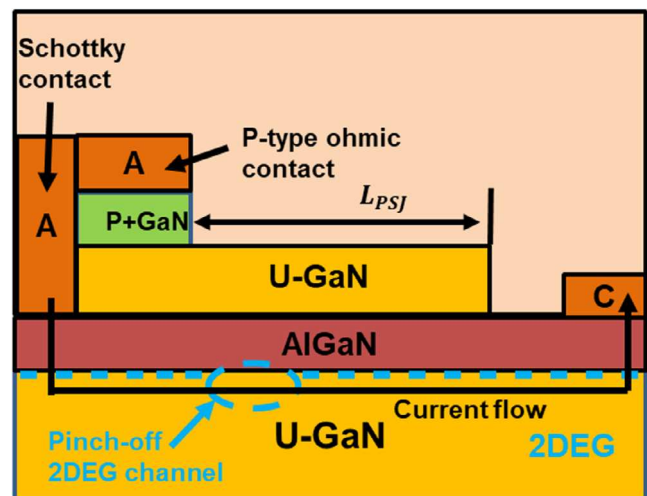
Figure 7. The mechanisms of current saturation behavior in PSJ hybrid diode.

Figure 8 illustrates the I–V characteristics as a function of temperatures from 25 to 150 °C with the step of 25 °C. The saturation current drops with the rise of temperatures. This is due to the decrease of the 2DEG mobility. Furthermore, the saturation voltage is almost consistent at different temperatures.

Based on the simulation analysis, the mechanisms of this current saturation behavior are based on the theory of velocity saturation. The saturation velocity as a function of temperature in AlGaN or GaN is reported in refs. [20,21]. It shows a marginally decreasing trend with the rise of temperature,[20,21] causing a slight reduction of saturation voltage. This trend is very similar to the relationship between the temperature and saturation voltage in PSJ hybrid diodes. Therefore, velocity saturation is a highly plausible theory of the current saturation of PSJ hybrid diodes, which is consistent with the analysis of HEMTs.

Figure 8. The measured I–V characteristics of PSJ hybrid diode as a function of temperature (from 25 to 150 °C with the step of 25 °C).

4. Conclusion

The current saturation behavior in the PSJ hybrid diode is first reported and discussed utilizing the device simulation tools. Although these are merged PiN-Schottky diodes, the PiN junctions do not turn on due to the low resistivity of 2DEG beneath this region. Therefore, the GaN PSJ hybrid diode behaves as a unipolar power device.

By comparing the potential distribution along the 2DEG and 2DHG channels, the mechanisms involved in the current saturation behavior are discussed. Along the 2DEG channel, the applied anode potential drop across the Schottky contact region is about 1 V in the saturation region. The drift region has a very low potential drop due to the high density of 2DEG, which keeps the potential of the L_{PSJ} region as low as possible. However, the potential drop along the 2DHG channel is different. The potential drop at the Ohmic contact and P-GaN layer is insignificant, but the rest of the applied anode voltage is dropped across the regions immediately adjacent to the edge of the p-GaN region toward the cathode. This significant potential drop occurs within a short distance, resulting in a high electric field and depletion of electrons. Therefore, a pinch-off region is created, which causes velocity saturation to occur at this region.

Conflict of Interest

The authors declare no conflict of interest.

Data Availability Statement

The data that support the findings of this study are available from the corresponding author upon reasonable request.

[1] O. Ambacher, J. Smart, J. R. Shealy, N. G. Weimann, K. Chu, M. Murphy, W. J. Schaff, L. F. Eastman, R. Dimitrov, L. Wittmer, M. Stutzmann, W. Rieger, J. Hilsenbeck, *J. Appl. Phys.* **1999**, *85*, 3222.

[2] M. Asif Khan, A. Bhattarai, J. N. Kuznia, D. T. Olson, *Appl. Phys. Lett.* **1993**, *63*, 1214.

[3] E. A. Jones, F. F. Wang, D. Costinett, *IEEE J. Emerg. Sel. Top Power Electron.* **2016**, *4*, 707.

[4] A. Nakajima, Y. Sumida, M. Dhyani, H. Kawai, S. Ekkanath Madathil, *Appl. Phys. Express* **2010**, *3*, 12.

[5] A. Nakajima, P. Liu, M. Ogura, T. Makino, K. Kakushima, S. I. Nishizawa, H. Ohashi, S. Yamasaki, H. Iwai, *J. Appl. Phys.* **2014**, *115*, 153707.

[6] A. Nakajima, P. Liu, M. Ogura, T. Makino, S. Nishizawa, S. Yamasaki, H. Ohashi, K. Kakushima, H. Iwai, *Appl. Phys. Express* **2013**, *6*, 091002.

[7] A. Nakajima, K. Adachi, M. Shimizu, H. Okumura, *Appl. Phys. Lett.* **2006**, *89*, 193501.

[8] A. Nakajima, Y. Sumida, M. H. Dhyani, H. Kawai, E. M. Narayanan, *IEEE Electron Device Lett.* **2011**, *32*, 542.

[9] A. Nakajima, M. H. Dhyani, E. M. S. Narayanan, Y. Sumida, H. Kawai, in *IEEE 23rd Int. Symp. on Power Semiconductor Devices and ICs*, San Diego, CA, USA **2011**, pp. 280–283.

[10] V. Unni, H. Y. Long, M. Sweet, A. Balachandran, S. Ekkanath Madathil, A. Nakajima, H. Kawai, in *2014 IEEE 26th Int. Symp. on Power Semiconductor Devices & IC's (ISPSD)*, Waikoloa, HI **2014**, pp. 245–248.

[11] A. Nakajima, V. Unni, K. G. Menon, M. H. Dhyani, E. M. Sankara Narayanan, Y. Sumida, H. Kawai, in *Proc. of the Int. Symp. on Power Semiconductor Devices and ICs*, Bruges, Belgium **2012**, pp. 265–268.

[12] H. Kawai, S. Yagi, S. Hirata, F. Nakamura, T. Saito, Y. Kamiyama, M. Yamamoto, H. Amano, V. Unni, E. M. S. Narayanan, *Phys. Status Solidi A* **2017**, *214*, 1600834.

[13] H. Yan, Y. Du, P. Luo, X. Tan, E. M. S. Narayanan, *IEEE Trans. Electron Devices* **2021**, *68*, 5714.

[14] L. Nela, C. Erine, A. M. Zadeh, E. Matioli, *IEEE Trans. Electron Devices* **2022**, *69*, 1798.

[15] L. Nela, C. Erine, M. V. Oropallo, E. Matioli, *IEEE J. Electron Devices Soc.* **2021**, *9*, 1066.

[16] A. Sheikhan, G. Narayanankutty, E. M. S. Narayanan, H. Kawai, S. Yagi, H. Narui, *Jpn. J. Appl. Phys.* **2023**, *62*, 014501.

[17] A. Sheikhan, S. N. Ekkanath Madathil, H. Kawai, S. Yagi, H. Narui, *J. Appl. Phys.* **2023**, *62*, 064502.

[18] Y. Du, H. Yan, P. Luo, X. Tan, E. M. S. Narayanan, H. Kawai, S. Yagi, H. Narui, *IEEE Trans. Electron Devices* **2023**, *70*, 178.

[19] V. Unni, H. Y. Long, H. Yan, A. Nakajima, H. Kawai, E. M. S. Narayanan, *IET Power Electron.* **2018**, *11*, 2198.

[20] R. Quay, C. Moglestue, V. Palankovski, S. Selberherr, *Mater. Sci. Semicond. Process.* **2000**, *3*, 149.

[21] A. F. M. Anwar, S. Wu, R. T. Webster, *IEEE Trans. Electron Devices* **2001**, *48*, 567.